ROYAL SOCIETY OF CHEMISTRY

TUTORIAL REVIEW

Check for updates

Fluorescence spectroscopy: detection and sensing of SO₂ and H₂S using MOFs and other emerging porous materials

Marco L. Martínez,[a,b] Pablo Marín-Rosas,[c] Valeria B. López-Cervantes,[a] Ariel Guzmán-Vargas,[b] Ricardo A. Peralta, [ID] *[c] Diego Solis-Ibarra [ID] *[a] and Ilich A. Ibarra [ID] *[a]

In this tutorial review we introduce the basic concepts on fluorescence spectroscopy as an analytical technique to detect and sense sulphur dioxide (SO_2) and hydrogen sulphide (H_2S), specifically, by using metal–organic frameworks (MOFs) and emerging porous materials *i.e.*, covalent organic frameworks (COFs) and porous organic cages (POCs) as fluorescent probes. Following a logical order, we present the basic concepts of fluorescence spectroscopy, origin of fluorescence in MOFs, a concise description of emerging applications of fluorescent MOFs, specific H_2S and SO_2 interactions with MOFs structures, and selected edge of science examples of MOFs, COFs and POCs as probes with special emphasis on the relationship between materials' chemical structure and fluorescence response. Finally, after each example, we describe the strategy employed to detect the specific analyte.

Key learning points

(1) A functional understanding of the basic concepts in fluorescence spectroscopy.
(2) Key ideas of MOFs fluorescence origin.
(3) Exploring the chemical and physical interactions between metal organic frameworks and SO_2, and H_2S.
(4) To understand and explain the different responses in MOF fluorescence emission after the exposure to toxic gases.
(5) To take further these concepts and knowledge to other porous materials (*e.g.*, COFs, and POCs).

1. Introduction

Fluorescence detection is extensively used due to the distinct advantages offered by this technique in terms of sensitivity, selectivity, and response time. For example, fluorescence methods provide lower limit of detections (LOD) than those of absorption methods.[1] Furthermore, many chemical and biochemical analytes can be detected by general fluorescence methods: anions (halide ions, citrates, carboxylates, ATP, *etc.*), cations (Li^+, H^+, K^+, Mg^{2+}, Cd^{2+}, *etc.*), neutral molecules, gases

(O_2, CO_2, NO, *etc.*), biological macromolecules (proteins, DNA, *etc.*) and biochemical analytes (amino acids, coenzymes, carbohydrates, nucleosides, nucleotides).[2] Since most analytes are not fluorescent, fluorescent probes are commonly used, which are materials or even small molecules that can interact in a specific way with the analytes. Examples of fluorescent probes range from small molecules such as coumarins, naphthalimides,[3] to more complex systems such as, functionalised carbon nanotubes, fluorescent polymers, sol–gel materials, silica-based mesoporous materials, and nanoparticles (*e.g.*, silica and polymer-based nanoparticles and quantum dots).[2]

Metal–organic frameworks (MOFs) are porous materials, constructed by joining metal cations or metal clusters, named secondary building units (SBUs), through organic linkers. MOFs feature superior specific area, permanent porosity, and, specially, ease to functionalisation by tuning the SBUs and/or organic linkers.[4,5] Interestingly, some MOFs also show high chemical and thermal stability under harsh conditions.[6–8] Due to these unique properties, these materials have been studied for widely applications, like catalysis,[9,10] energy storage,[11,12] gas capture,[13,14] and fluent-gasses separation.[15,16] Thus, some

[a]Laboratorio de Fisicoquímica y Reactividad de Superficies (LaFReS), Instituto de Investigaciones en Materiales, Universidad Nacional Autónoma de México, Circuito Exterior s/n, CU, Del Coyoacán, 04510 México D.F., Mexico. E-mail: diego.solis@unam.mx, argel@unam.mx
[b]Laboratorio de Investigación en Materiales Porosos, Catálisis Ambiental y Química Fina, Instituto Politécnico Nacional, ESIQIE-SEPI-DIQI, UPALM Edif. 7 P.B. Zacatenco, GAM, 07738 CDMX, Mexico
[c]Departamento de Química, División de Ciencias Básicas e Ingeniería, Universidad Autónoma Metropolitana-Iztapalapa, San Rafael Atlixco 186, Col. Leyes de Reforma 1ra Seccion, Iztapalapa, 09310 Ciudad de Mexico, Mexico. E-mail: rperalta@izt.uam.mx

metal–organic frameworks have shown luminescent properties,[17,18] therefore, giving these materials the potential to be used as probes for fluorescent detection. Lately, the research on the use of MOFs as probes for different chemical species has become a hot topic. For example, the sensing and detection of cations, anions, different molecules, and gasses, have been extensively reported.[19–21]

Further to the greenhouse gases, ammonia (NH_3) carbon monoxide (CO), sulphur dioxide (SO_2), volatile organic compounds (VOCs), and hydrogen sulphide (H_2S) are some of the most hazardous air pollutants.[22] SO_2 is a highly corrosive toxic gas, which can be easy absorbed by dermal contact or easily inhaled into the respiratory system. Human contact to sulphur dioxide can cause drastic respiratory difficulties, principally in lung function (*i.e.*, broncho-constriction), and direct contact over 100 SO_2 ppm becomes deadly.[23] Additionally, H_2S is a colourless gas which is flammable, also extremely corrosive, and toxic to human beings, specifically, concentrations around 100 ppm can instantly numb the olfactory nerve, and concentrations above 700 ppm become deadly.[24]

2. Fluorescence phenomenon

2.1. Basic concepts on fluorescence

When a molecule is exposed to photons with suitable energy, they are promoted from ground state to electronically excited state. Light excitation generates changes in the electronic

Ilich A. Ibarra (left), Ricardo A. Peralta (middle) and Diego Solis-Ibarra (right)

Ilich A.Ibarra is a Full Professor at UNAM working on the use of MOFs for the capture and detection of toxic gases such as SO_2 and H_2S. Ricardo A. Peralta is a Full Professor at UAM who is interested on novel catalytic application of semi-open metal sites within MOFs. Diego Solis-Ibarra serves as the Director of the Institute for Materials Research at UNAM, and his research focuses on hybrid materials for sensing, photovoltaics, and optoelectronics.

structure of a molecule so that excited states species have their own electronic structure, different from that one of the ground state. Molecular ground state is responsible for the absorption spectrum. On the other hand, the excited states are responsible for deactivation processes which involve energy loss processes, either radiative (luminescence) or non-radiative. Electronically excited states own high-energy content and, therefore, must suffer deactivation within a short time. Because of the Franck–Condon principle, light absorption usually generates the excited state in high vibrational level, as well as light emission generates the ground state in the high vibrational level.[25] In this context, we will only deal with the luminescence which is produced by deactivation of excited state species produced by photon irradiation.

As we described before, luminescence is the spontaneous radiative deactivation, *i.e.*, there exist emitted photons. Difference between fluorescence and phosphorescence stands in spin multiplicity and the intrinsic time of both processes. Specifically, in fluorescence phenomenon, the spin multiplicity, normally found in singlet state in the ground state, is conserved, *i.e.*, the excited state possesses a singlet state. Conversely, in phosphorescence there is a change in spin multiplicity, from singlet in the ground state, to triplet in the excited state. This change in spin multiplicity is known as intersystem crossing. Intersystem crossing is a not allowed electronic transition; therefore, phosphorescence presents higher decay time. Additional to fluorescence and phosphorescence, excited state species can also deactivate *via* vibrational relaxation, when "colliding" with surrounding species. Similar to vibration relaxation, excited molecules can undergo intramolecular vibration redistribution, meaning that the energy originally localised in the mode populated light absorption is rapidly spread among the other vibration modes.[25] This becomes important in large molecules which can present several vibrational modes, giving as consequence that limited photons are emitted.

Different chemical species can exhibit fluorescent properties such as organic molecules,[26] inorganic complexes,[27] and semiconductor materials (*e.g.*, quantum dots,[28] carbon dots,[29] perovskites).[30] Regarding metal–organic frameworks, having insights into fluorescent features of their organic molecular constituents can be critical to understand their emission behaviour. Additionally, as we shall see in section 5, new emerging materials built up from pure organic building blocks have shown outstanding detection and sensing towards both SO_2 and H_2S. Organic molecules present a direct relationship between their fluorescent properties and their structure. For example, generally, a shift of the absorption and fluorescence spectra to longer wavelengths is a result of an increase in the extent of π-electron system. Molecules with extended molecular systems exhibit remarkable emission intensity, which arise as result of their highly efficient π → π* transitions, possessing high molar absorption coefficients and high fluorescence quantum yields.[31,32] If molecules with π systems have also heteroatoms within their structure, additional n → π* transitions appear as, normally, the lowest

lying transition. These $n \rightarrow \pi^*$ transition possess lower quantum yields that those of $\pi \rightarrow \pi^*$ transitions.[25]

2.2 Origins of fluorescence in MOFs

The sources of fluorescence signals in metal–organic frameworks can be classified into ligand, charge transfer, metal centres, and guest molecules sources:[33,34]

Ligand-centred fluorescence. If there is no substantial charge transfer (CT), *i.e.*, an electron "movement" from an orbital to another, or resonance energy transfer (RET), which means an optical process, in which the excess energy of an excited molecule (donor) is transferred to an acceptor molecule, between ligand and the metal centre, MOF's fluorescence behaviour is very similar to the fluorescence of the organic ligand in terms of emission wavelength and spectral shape. Charge transfer between metal and ligand can be divided as ligand-to-metal charge transfer (LMCT) *i.e.*, electron moves from ligand to metal, and metal-to-ligand charge transfer (MLCT) which means electron movement from metal to ligand. If LMCT or MLCT exists within the MOF structure, the energy level of the ligand is slightly disturbed, and the emission wavelength shifts (red shift for MLCT and blue shift for LMCT). Additionally, LMCT and MLCT generates a change in emission intensity in comparison to intrinsic ligand fluorescence. Sometimes there can be CT or RET between ligands, or even different parts of the same ligand, namely, ligand-to-ligand charge transfer (LLCT) or ligand-to-ligand resonance energy transfer (LLRET). Additionally, it has been observed in MOF materials, that, upon coordination between ligand and metal centres, vibrational rotations are diminished, which lead to a "rigidization" of the framework structure, and, as consequence, an enhancement in emission intensity. In summary, for the ligand-centre fluorescence, fluorescence arises as a result of purely ligand-related electronic transitions, mainly ascribed to $\pi^* \rightarrow n$, $\pi^* \rightarrow \pi$ or other possible transfers of π-conjugated aromatic ligands, which can be altered by CT and RET phenomenon.

Charge transfer fluorescence. When the energy gap between the lowest unoccupied molecular orbital (LUMO) and the highest occupied molecular orbital (HOMO) in organic ligand is considerable, it is more feasible for LMCT and MLCT to happen. LMCT takes specifically relevance in Co^{2+}, Ni^{2+} Cu^{2+}, Cd^{2+}, Zr^{4+}, Ti^{4+}, and Fe^{3+}-based MOFs. On the other hand, MLCT is typically observed in electron-fully-filled Cu^+, and Ag^+-based MOFs, where π-acid ligands offer empty orbitals to facilitate charge transfer. In this case, fluorescence appears upon luminescent deactivation related to LMCT or MLCT transitions.

Metal-centred fluorescence. This fluorescence source is commonly found in lanthanide-based MOFs, where organic ligands can sensitise lanthanides *via* ligand-to-metal resonance energy transfer (LMRET), also known as "antenna effect". The antenna effect is necessary to this source of fluorescence, since lanthanides have low luminous efficiency due to the f–f transition inhibition.
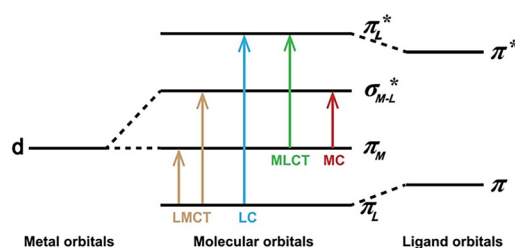

Fig. 1 Simplified diagram illustrates different types of electronic transitions in photoluminescent MOF. (Reproduced from ref. 34 Copyright 2025 with permission from Elsevier).

Guest induced-based fluorescence. Since metal–organic frameworks possess permanent porosity, guest fluorescent molecules or species can be loaded into these MOFs. Some examples are lanthanide ions, dyes, and precious metal complexes.

Fig. 1 shows the possible different electronic transitions in photoluminescent metal–organic frameworks, where LMCT, LC, MLCT and MC stands for ligand-to-metal charge transfer, ligand-centred, metal-to-ligand charge transfer, and metal-centred transitions.

2.3 Fluorescent MOFs applications

Additional to detection and sensing, which is the main theme presented in this tutorial review, photoluminescent metal–organic frameworks have been evaluated to several applications. For instance, some metal–organic frameworks show upconversion, defined as a phenomenon where a material absorbs photons of lower energy (longer wavelength) and emits photon of higher energy (shorter wavelength). Upconversion materials stands importance since this phenomenon can be used in emerging technologies such as photocatalyst, luminescence imaging, optogenetics, anti-counterfeiting technology, photo-switching, 3D printing, solar cells, organic light-emitting diodes, night-vision devices, deep-penetrating photodynamic therapy, and disease treatments. In this regard, lanthanide-based MOFs have raised its relevance for presenting upconversion, generally, *via* energy transfer,[35,36] see section 4 for a concise energy transfer explanation.

MOFs which do not possess upconversion phenomenon have also demonstrated intriguing fluorescent features as result of their highly tuneable structure. A remarkable example was introduced by Uribe-Romo *et al.*,[37] where the authors studied metal–organic frameworks which show multicolour emission. Multicolour emission is a phenomenon mostly found in solution state where multiple emitters are dissolved. In solution state, this phenomenon can be easily managed since exact concentration of emitters can be controlled. On the other hand, in crystalline solid state, organic-based multicolour emission is challenging, because when solvent is removed, the organic fluorophores tend to aggregation, and phase separation, leading to unpredictable and low fluorescence intensities. Multicolour emission has been developed in crystalline solid state using the concept of substitutional
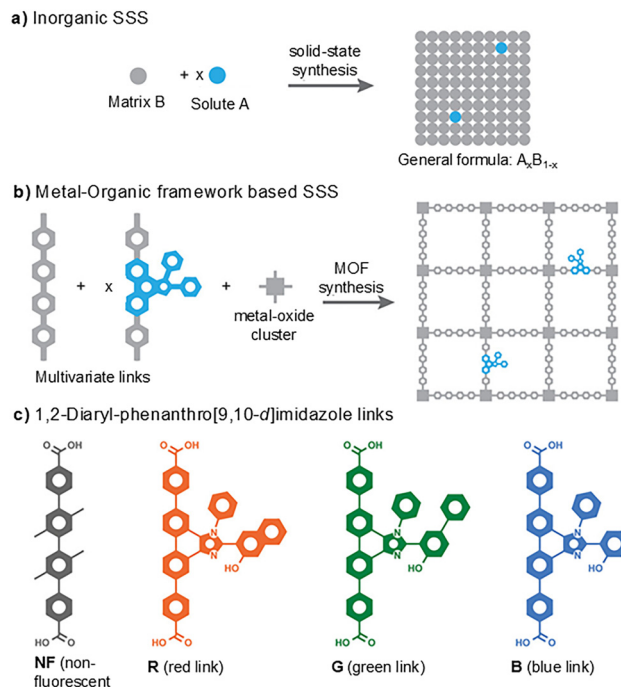
Fig. 2 Schematic representation of (a) inorganic substitutional solid state (SSS), and (b) metal–organic framework based SSS; (c) linkers which are non-fluorescent and emit photons at red (R), green (G), and blue (B) wavelength. (Reproduced from ref. 37 Copyright 2019 with permission from American Chemical Society).

solid solutions (SSS). In inorganic materials, SSS are easily obtained because inorganic materials deal with atoms disposed in exact atomic positions (Fig. 2a). In contrast, for organic materials, SSS are more complicated to form, since unlike atoms, organic molecules are not spherical, thus, matrix-dopant matching is a nontrivial assignment. Within this context, Uribe-Romo and coworkers used the outstanding properties of MOFs, specifically, the predictable crystallographic positions of linkers in the MOF crystal. The authors employed the concept of multi-variate links, which is simply defined as the substitution of linkers in the same MOF (Fig. 2b), to create metal–organic frameworks which emits at different wavelengths. Thus, they obtained different emission colours based on the pre-synthetic selection and concentration control of the linker and the substitutional linkers, i.e., a non-fluorescent linker (NF), and linkers which emit at red (R), green (G) and blue (B) colours, see Fig. 2c. Applications of multicolour emission, based on crystalline materials, are found in lasers and blue LEDs.[38,39] Hence, metal–organic frameworks broad the possibility to develop new concepts and applications in fluorescence technologies by merging both organic and inorganic materials.

3. Interaction of MOFs with SO_2 and H_2S

One of the most studied fields in MOFs are the diffusion phenomenon and host–guest interactions. Solvent molecules

derived from the synthesis (such as water or dimethyl-formamide) can be found as guests in the framework of the material. Gas adsorption studies have demonstrated that other molecules (e.g., CO_2, CH_4, SO_2 or H_2S) can be trapped inside the MOF due to the porosity and high surface area of the materials. Different strategies have been reported for the improvement of these host–guest interactions, such as ligand functionalization, variation of metal centres and generation of defects.[40] However, several studies focus on understanding these interactions through different characterization techniques. In 2018, Caro and coworkers presented the interaction between different molecules and Co-MOF-74.[41] The sensing performance of the MOF was evaluated for different molecules (Ar, CO_2, propene, propane, MeOH and H_2O), where the obtained Vis/NIR absorption spectra presented interesting insights in the interaction of these molecules and the framework. Minor interaction was found for Ar and propane; however, a shift in the absorption band was observed for propene and CO_2 due to the interaction of the Co centre in the MOF and the functional group (double bond or oxygen atom) present in the guest molecule. A significant shift was presented for the MeOH, and H_2O sample, this was attributed to the interaction of the metal centre with the oxygen atom in the molecule and an additional hydrogen bond formed between the organic linker in the MOF and the hydrogen atom present in the guest molecule. Raman spectroscopy presented a shift in the C=O stretching peak (~ 1250 cm^{-1}) and the O–C–O-symmetric stretching peak (~ 1450 cm^{-1}) depending on the gas exposure. These results confirmed the different interactions between the Co-MOF and the exposed molecules, demonstrating the activity of Co-MOF-74 as a gas sensor.

An interesting approach is presented, where the MOF thin film is synthetized layer by layer directly on modified substrates, called SURMOFs (surface-anchored metal–organic frameworks). SURMOFs have controllable thickness, higher crystalline orientation and a lower defect density, which presents an advantage for optical and sensing applications.[42] Knebel et al. studied the synthesis of MIL-68(In) thin films on Au-surfaces for optical cavity sensing.[43] The material was exposed to N_2, EtOH and toluene, where the UV-vis spectra presented changes in the characteristic signals that demonstrated selectively detecting chemical gases. EtOH and toluene showed a red shift in the spectra due to the increasing the density in the pores of the material, when N_2 is used a blue shift is observed. These results presented an interesting alternative for optical sensors. Other example, presented by Amador-Sánchez and coworkers,[44] utilized X-ray photoelectron spectroscopy, to visualize interactions between UTSA-16(Zn) and sulphur dioxide. Specifically, the authors were able to stablish the framework–SO_2 interactions by changes in binding energies of the C, K, and O atoms interacting with SO_2. Thus, these examples, demonstrate how selected analytical techniques are used to precisely study MOF–guest interactions, which are important to have better insights about selective fluorescence detection/sensing.

In order to have a better perspective on MOFs which can be used in fluorescence detection towards SO_2, and H_2S, it is important to have insight into the interactions between these analytes and the constituents composing metal–organic frameworks. First, it is necessary to have insight into the physico-chemical properties of both sulphur dioxide and hydrogen sulphide. SO_2 (Fig. 3a) shows a bent geometry with an angle of approximately 120° between the central sulphur and both peripheral oxygen atoms. The bonding consists in a covalent S=O double bond and an ionic S^+–O^- bond leading to a resonance effect (bond length = 1.43 Å) This molecule is polar with a 1.63 D dipole moment.[45,46] Additionally, oxygen, an electron-rich atom, can function as Lewis base, whereas sulphur can be a Lewis acid site. Regarding H_2S (Fig. 3b), it also exhibits a bent geometry (H–S–H angle = 92.4°) with a bond length (S–H) of 1.33 Å.[47] The dipole moment value of this molecule is 0.97 D.[48]

Therefore, since both molecules are polar, they can interact, as host molecules, with either inorganic nodes or functional groups (*vide infra*) within the MOF structure. Specifically, metal–organic frameworks possess different chemical functionalities, such as coordinatively unsaturated sites (CUS) (also known as open metal sites (OMS)), and other functional groups (*e.g.*, μ-OH groups), which control and establish specific host–guest interactions. As seen in Fig. 4, general host–guest interactions in MOF systems include van der Waals forces, hydrogen bonding, electrostatic forces and coordination bonding, where coordination bonding stands as the stronger interactions among them.[49]

In this regard, for SO_2 and H_2S-MOF interactions, the most important functional groups are CUS, μ-OH, –NH_2 groups, defective sites, and halogen groups. Additionally, SO_2 and H_2S can also interact with phenyl, and C–H groups.[8,50]

Thus, we aim to introduce basic concepts that will help to have a better understanding of SO_2 and H_2S interactions with MOFs and, consequently, fluorescence detection towards both analytes:

Coordinatively unsaturated sites:[51,52] the concept of free coordination sites is well established in classical coordination chemistry, in which free coordination sites appear in complexes with a lower number than the common coordination number of the metal atom. Additionally, in contrast to OMS in MOFs, in classical coordination chemistry "free coordination sites" often appear only as intermediary or transition states. This is due to CUS are occupied by labile solvent molecules, since coordination chemistry or catalysis is often conducted in solution-state. For MOFs, metal coordination sites and the pores of a MOF is typically filled by the solvent which was used in the synthetic procedure. This occurs when metal ions are not solely coordinated to the donor atoms of the bridging ligands, in order to saturate their coordination sphere. The procedure to remove the labile solvent molecules coordinated to metal centres, generating at the same time CUS, generally termed "activation", is usually solvent exchange and removal (Fig. 5).[53] The relevance of CUS stands since these can act as Lewis acid sites, where host molecules, such as H_2S, and SO_2, can coordinate.

Electrostatic interactions: polar host–molecules can interact with different partially charged functional groups present in a particular MOF material.

Hydrogen bonding: A hydrogen bond may be considered as a specific kind of dipole–dipole interaction in which a hydrogen atom, attached to an electronegative atom (or electron-withdrawing group), is attracted to a neighbouring dipole on an adjacent molecule or functional group. Hydrogen bond is normally written D-H⋯A, in where D, and A represent donor and acceptor atoms, respectively, the solid line is the covalent bond, and the dashed line is the hydrogen bond.[54]

In this regard, in the following section we present selected examples of the interactions between SO_2 and H_2S. It is worth to mention that both sulphur dioxide and hydrogen sulphide, due to their corrosive properties, can "break" the MOFs structure, principally, by breaking the coordinate bond between ligands and metal centres.[55] Accordingly, several approaches have been applied to obtain MOFs with high stability towards both SO_2 and H_2S. For example, the employment of robust
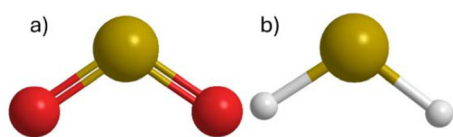

Fig. 3 (a) Sulphur dioxide molecule (SO_2), and (b) hydrogen sulphide molecule (H_2S); colour code: S = yellow, O = red, H = white.
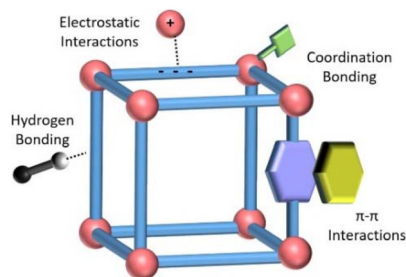

Fig. 4 Schematic representation of guest molecules-MOFs interactions (reproduced from ref. 49 Copyright 2025 with permission from Elsevier).
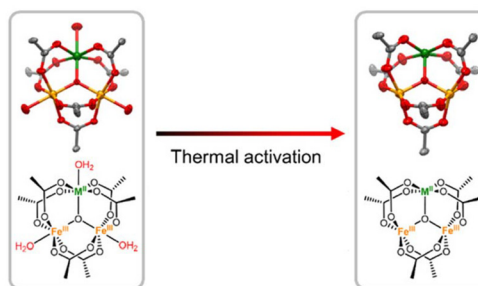

Fig. 5 Creation of open-metal sites upon thermal activation in PCN-250(Fe$_2$M): oxygen = red, Fe = gold, metal atom = green, Carbon = grey (reproduced from ref. 53 licensed under CC-BY 4.0).

metal-linker bond, the use of inert or higher-valent centre metals (*e.g.*, Al^{3+}, Cr^{3+}, Zr^{4+}), and the utilisation of SBU with poly-nuclear nature, since multinuclearity provides, theoretically, enhanced thermal and chemical stability.[13,50] Respecting the use of higher-valent ions, these allow the formation of strong M–O bonds compared to divalent ions. Additionally, as we shall see, hydrogen sulphide might form strong bonds with the framework, *i.e.*, metal–sulphur bond, generally irreversible, which can compromise the chemical stability of MOFs. With this drawback in mind, MOFs constructed with SBUs which possess μ-OH functional groups can established hydrogen bonds with hydrogen sulphide, thus moderating the MOF-H_2S interaction leading to chemical stability enhancement.[50] Nevertheless, the reactivity of H_2S with metal centres can be used as smart strategy to selective sense hydrogen sulphide, see section 4.2.

3.1 SO_2 and H_2S-MOF interactions

As previously mentioned, open metal sites can function as Lewis acid sites, making these metal centres capable of coordinating with SO_2 through oxygen atoms. For example, Morris *et al.*[56] demonstrated, by *in situ* single-crystal X-ray diffraction (scXRD) studies, that SO_2 can be both chemisorbed and physisorbed on MOF-74 (also known as CPO-27), where SO_2 coordinates to Ni^{2+} open metal sites (Fig. 6). MOF-74 family shows high density of open metal sites within its internal pore environment. The M^{2+} ions are connected by 2,5-dihydroxylterephthalaate linkers (2,5-dhtp) into a porous structure. It contains one-dimensional hexagonal channels along the crystallographic *c*-axis.[57] After thermal activation, these channels contain open metal sites. Specifically, Morris and coworkers activated a single crystal at 450 K under vacuum conditions

until a residual occupancy of M–O_{water} (Ow) was down 11%. Then, SO_2 was hosted to the sample at 450 K and 2 bar. Under these conditions, SO_2 binds to Ni(II) open metal sites, through one of the oxygen atoms. Finally, reducing the temperature to 300 K while maintaining the same SO_2 pressure produced two effects. First, it increased the amount of metal bound SO_2, and second, the reduction in temperature afforded some SO_2 physisorbed, see Fig. 6.

Xing and coworkers[58] studied the binding sites of sulphur dioxide with SIFSIX-1-Cu framework. SIFSIX-1-Cu comprises Cu^{2+} metal ions coordinated to SiF_6^{2-} building blocks which are pillared through 4,4′-bipyridine ligands. Based on first-principles of DFT calculations, they found out that SO_2 gets adsorbed primarily through $S^{\delta+}\cdots F^{\delta-}$ electrostatic interactions (Fig. 7) with the SiF_6^- anion and the multiple $O^{\delta-}\cdots H^{\delta+}$ dipole–dipole interactions from the 4,4′-bipyridine linker (Fig. 7b). The DFT-D estimated a S⋯F distance of ≈2.6 Å (Fig. 7a), significantly smaller than the sum of the van der Waals radii of S and F (3.3 Å), pointing out the considerable strength of this interaction that arises from the negative nature of the SiF_6^{2-} ion and positive charge of S atom. At the same time, the two oxygen atoms from the sulphur dioxide molecule are bonded by the 4,4′-bipyridine linker *via* multiple dipole–dipole interactions, especially the $O^{\delta-}\cdots H^{\delta+}$ interactions between the oxygen atoms and aromatic hydrogens with a distance of 2.39–3.30 Å (Fig. 7b).

On the same way that SO_2, H_2S can also coordinate to open metal sites present in metal–organic frameworks. HKUST-1 is a prototypical MOF built up by dimeric Cu^{2+} paddle wheel SBU which are connected *via* benzene-1,3,5-tricarboxylate (BTC) linkers. Interestingly, HKUST-1 can provide CUS, normally, by an activation procedure, see Fig. 8a and b.[59] Bandosz *et al.*,[60] studied the adsorption of H_2S on HKUST-1 and HKUST-1/graphene oxide composites. According to their results, although HKUST-1 shows a competitive H_2S capacity, *i.e.*, 92 mg g^{-1}, this material losses its porosity as well as its crystallinity after the exposure to hydrogen sulphide. They attributed this phenomenon to the formation of CuS species, as a consequence of a sequential chemical reaction, wherein the first
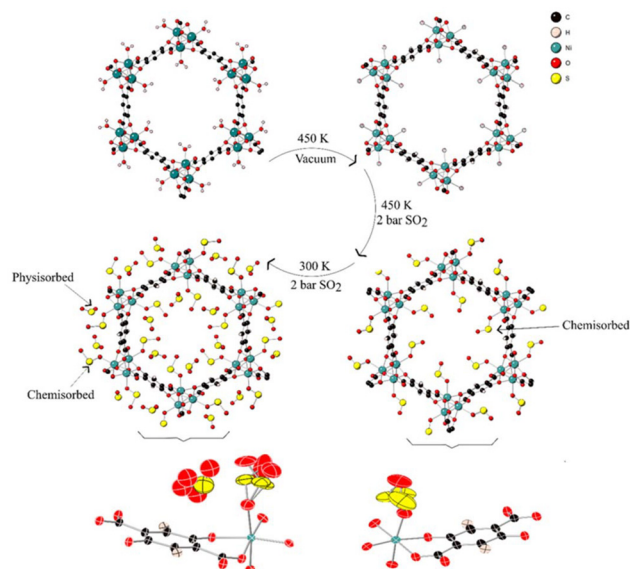

Fig. 6 Different stages of chemisorbed and physisorbed SO_2 on MOF-74 open channel (reproduced from ref. 56 licensed under CC-BY 4.0).
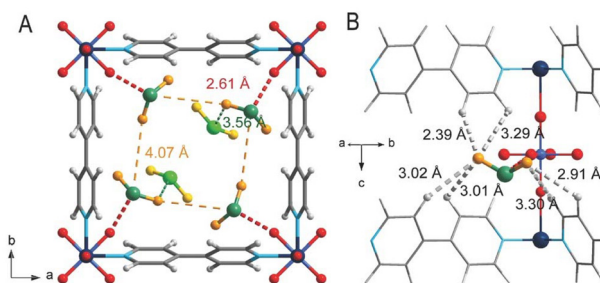

Fig. 7 (A and B) DFT-D calculated SO_2 adsorption binding sites in SIFISX-1-Cu viewing in two different directions. Colour code: F = red; Si = light blue; C = grey; H = light grey; N = sky blue; Cu = dark teal; O = orange; S = sea green. The secondary adsorbed SO_2 molecules were highlighted with bright colour (Reproduced with permission from ref. 58 Copyright 2017 with permission from John Wiley and Sons).
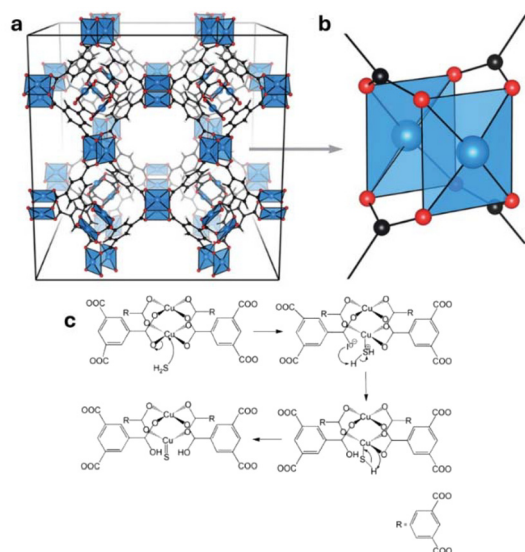
Fig. 8 (a) HKUST-1 crystal structure, (b) paddlewheel secondary building units (reproduced from ref. 59 licensed under CC 3.0), and (c) proposed mechanism of the reaction between H_2S and Cu open metal sites, forming CuS species (reproduced from ref. 60 Copyright 2010 with permission from John Wiley and Sons).

step is the adsorption of H_2S on Cu(II) coordinatively unsaturated sites (Fig. 8c). Additional to this example, H_2S can also react with metal centres within MOF structures to form polysulfides species,[61] which, can be used as a smart strategy to detect hydrogen sulphide selectively, *vide infra*.

4.   MOFs for SO_2 and H_2S detection and sensing

Depending on the electronic nature of the introduced analyte and the photoluminescent behaviour of the MOF probe, MOF-based sensors usually exhibit three main responses on the emission spectra: (i) "turn-off", (ii) "turn-on", and (iii) shift of the emission. Additionally, there are also reports on fluorescence detection based on decay lifetime responses.[34] The former refers to a decrease on emission intensity of the probe after it interacts with the analyte, whereas the term "turn-on" means an increment on emission intensity *i.e.*, fluorescence enhancement as result of probe–analyte interactions as seen in Fig. 9. These probe–analyte interactions should generate electronic changes in the MOF in order to have a fluorescent response. Additionally, as we described in section 2.1, vibrational energetic levels can also play an important role in the probe fluorescent behaviour.

Regarding turn-off responses, the two most important types of interaction of an excited species with other molecules, which lead to emission intensity decrease, are electron-transfer and energy-transfer. Such processes manage to "quench" the excited state probe. The term quenching arises from the fact that they compete with the intramolecular deactivation paths
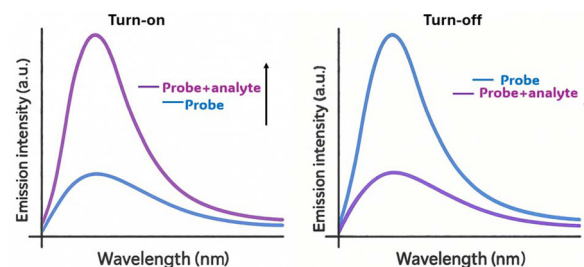

Fig. 9 Turn on, and turn-off fluorescence spectroscopy responses.

of excited species and, therefore, manifest themselves by quenching the intrinsic luminescence.[25] Energy-transfer (EnT) phenomenon, which can be simply defined as the transfer of excited-state energy from the donor to a ground-state acceptor in the neighbour, resulting in a simultaneous deactivation of the donor's energy and excitation of the acceptor's energy, has become of special interest in the use of MOFs as fluorescent probes.[62,63] EnT can be depicted as D* + A → D + A*, where the asterisk represents the excited state of the donor (D) and acceptor (A). According to their transfer mechanism, EnT can be categorised in two main groups, namely Förster resonance energy transfer (FRET) and Dexter energy transfer. FRET is based on weak dipole–dipole interactions between the acceptor and donor, providing long-range action (1–10 nm). Conversely, Dexter mechanism requires an acceptor-donor orbital wavefunction overlap, therefore, occurring at lower distances that FRET, less than 1 nm. Specifically, for MOFs, energy transfer processes are commonly divided into linker-to-linker energy transfer, linker-to-metal energy transfer, metal-to-metal energy transfer and MOF–guest energy transfer. In all cases, except for MOF–guest energy transfer, the transfer occurs within the same MOF structure. Nevertheless, although MOF–guest EnT takes major importance in sensing applications, just few reports have explicitly studied EnT mechanisms for SO_2 and H_2S detection.[64]

Quenching is generally classified as static or dynamic (collisional), in which static quenching occurs due to the formation of a non-fluorescent complex in the ground-state (*i.e.*, before excitation) between the fluorescent probe and the quencher. Dynamic quenching, in contrast, refers to collisions between fluorescent probes and quencher molecules after excitation. In the case of static quenching, the formation of the non-fluorescent complex in the ground state leads to less available probe species which can be excited, thus, generating lower concentration of excited-state species, and consequently less fluorescence (emission) intensity, since fluorescence intensity is directly related to excited-state species concentration. Additionally, since the probe retains its chemical composition, and lifetime (also known as decay time) measurements does not depend on excited-state species concentration, excited-state decay time is not modified, *i.e.*, probe's decay time is conserved. Furthermore, static quenching can also change emission maximum in fluorescence spectra. On the other hand, for dynamic quenching the probe–quencher interaction occurs

after excitation, adding extra non-radiative decay pathways, changing the probe original fluorescence lifetime. Thus, a way to distinguish between both quenching phenomena is by analysing fluorescence decay time, since static quenching does not generate significant changes in the fluorescent probe decay time.

On the other hand, turn-on responses generally arise as result of three different phenomena, that is, (i) the analyte acts as a new antenna molecule for the luminescent system, (ii) the analyte increases the rigidity of the MOF structure, inhibiting the non-radiative deactivation of excited state, and (iii) the analyte species facilities energy transfer and increases the absorption efficiency.

It is worth mentioning that, generally, two approaches are employed in order to detect/sense both SO_2 and H_2S, (i) direct measurement of H_2S and SO_2 species, and (ii) the use of ionic species, normally dissolved in water, as sources of H_2S and SO_2. The former involves the use of gaseous or dissolved SO_2 and H_2S in organic solvents. The second approach use inorganic salts as sources of SO_2 and H_2S. Regarding H_2S, the most common salts are NaHS, and Na_2S, which, when get in contact with water, react to form H_2S.[65] In the case of SO_2, the most common salts utilised are Na_2SO_3 and $NaHSO_3$.[66]

4.1 SO₂ detection and sensing

In 2023 Solis-Ibarra *et al.* reported the use of a chemically stable Ni(II)-MOF to address the difficult task of detecting SO_2.[67] Specifically, they used the MOF-type Ni_2(dobpdc), which is constructed from the coordination of Ni^{2+} ions and 4,4′-dioxidobiphenyl-3,3′-dicarboxylate (dopbdc)$^{4-}$ ligand. Ni(II) centres are hexa-coordinated to two bridging (μ_2) aryloxide O atoms from two different dobpdc ligands, see Fig. 10a. Since Ni_2(dobpdc) is a MOF-74 analogous material, Ni_2(dobpdc) possesses open metal sites, which appear after an activation process. Regarding SO_2 fluorescence detection, the

Ni_2(dobpdc) emission spectrum, upon the exposure to gaseous SO_2 at 1 bar, shows an increase in emission intensity compared to an activated sample, *i.e.*, Ni_2(dobpdc) exhibits a turn-on response. Furthermore, Ni_2(dobpdc) demonstrated good selectivity toward SO_2, since the exposure to CO_2 and water vapour at 1 bar practically did not change the intensity emission compared to activated sample, see Fig. 10a. Based on time-resolved photoluminescence (TRPL) experiments (Fig. 10b), Solis-Ibarra and coworkers suggest that SO_2 coordinate to Ni(II) centres, rigidifying the molecular motions of the organic ligand, which, subsequently, hinders non-radiative decay pathways of the photoexcited state, causing the fluorescence lifetime to slow down. Therefore, it increases the number of radiatively decaying excited species, generating an improvement in the fluorescence intensity. In this case, the fluorescence detection strategy consisted in taking advantage of the Ni(II) open metal sites, which allow SO_2 coordination, leading to rigidisation of the framework, enhancing the emission intensity.

Porphyrin-based metal–organic frameworks (PMOFs) have been extensively investigated as probes in fluorescence sensing for anions, cations, and other environmental pollutants.[68,69] Fluorescence properties in PMOFs arise as result of the extended π-conjugated systems in the organic ligand. In this regard, Horcajada and coworkers[70] investigated a highly porous hafnium cobalt–porphyrin tetracarboxylate MOF entitled (Hf)PCN-224(Co), therefore, reporting for the first time the employment of a porphyrin-based MOF for the SO_2 detection and sensing. (Hf)PCN-224(Co) comprises $Hf_6(OH)_8$ clusters linked by six square planar cobalt-metalated 5,10,15,20-tetrakis(4-carboxyphenyl) porphyrin, TCPP(Co) (Fig. 11a). In this study, the absorption spectrum of (Hf) PCN-224(Co) presents the characteristic electronic transitions for porphyrin molecules, *i.e.*, Soret band (or B band) and
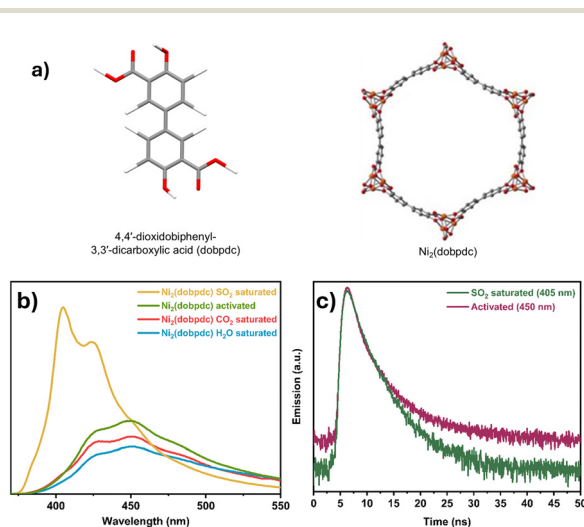

Fig. 10 (a) Structure of linker and Ni(dobpdc), (b) selective response of Ni(dobpdc) towards SO_2, and (c) decay-time of activated and SO_2 saturated samples (reproduced from ref. 67).
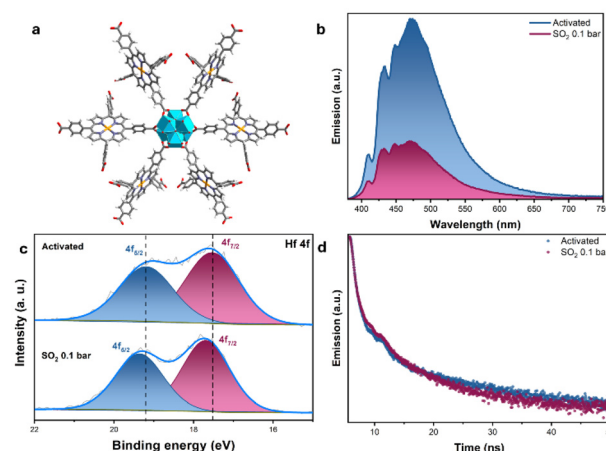

Fig. 11 (a) $Hf_6(OH)_8$ clusters coordinated to 6 TCPP(Co) linkers (C = grey, O = red, N = purple, H = white, Hf = blue, Co = gold), (b) turn-off response of gaseous SO_2, (c) turn-off responses of solution-state SO_2 at different concentrations, and (d) decay time measurements of (Hf) PCN-224(Co) activated and exposed to SO_2 at 0.1 bar. (Reproduced from ref. 70 licensed under CC-BY 4.0).

Q-bands. However, since the emission maximum wavelength is observed around λ_{em} = 475 nm (lower wavelength that Q-bands), it was suggested that the fluorescence phenomenon arises as result of LMCT transitions between TCPP(Co) and $Hf_6(OH)_8$ clusters. (Hf)PCN-224(Co) exhibited a turn-off response after the exposure to SO_2 at 0.1 bar, see Fig. 11b. Additionally, based on a solution-state experiment, a turn-off response was also observed as function of the SO_2 concentration, wherein a limit of detection of 175.5 ppm was obtained. Horcajada *et al.* proposed that SO_2 molecules interact strongly with the Hf(IV) centres, which was confirmed by X-ray photoelectron spectroscopy (XPS) (Fig. 11c), computational calculated Gibbs free energy of adsorption, and electron localisation function (ELF). Electronically, this strong SO_2–Hf(IV) interaction limits the LMCT electronic transitions responsible of (Hf)PCN-224(Co) fluorescence, leading to less excited-state species, therefore, leading to lower emission intensity, *i.e.*, turn-off response. In other words, the strong SO_2–Hf(IV) interactions form a non-fluorescence complex in the ground state, as can be seen in TRPL experiments (Fig. 11d), where, practically, there are no lifetime changes in the activated sample and the exposed to SO_2 at 0.1 bar sample. For (Hf)PCN-224(Co), the detection approach consisted in, once understanding the origin of fluorescence, that is, LMCT transitions, take advantage of Hf(IV) centres which are capable of strongly interact with SO_2, to limit the excited-state species formation.

4.2 H₂S detection and sensing

As we mentioned in section 3.1, coordinatively unsaturated sites can function as catalytic sites to react with hydrogen sulphide. An elegant example of using the reactivity of metal–organic frameworks with H_2S in order to detect H_2S was presented by Peralta and coworkers,[71] where they use SU-101 to form polysulfides species. SU-101 (Fig. 12a) is a Bi(III)-based MOF coordinated with ellagic acid ligands, where each Bi(III) metal centre is six coordinated, creating three bonds with co-ordinated phenolates, two μ_4-oxygens, and a coordinated water molecule, which can be removed by an activation process. Interestingly, the H_2S adsorption on SU-101 generates polysulfides *via* a catalytic process. Since the emission intensity of SU-101 showed a decrease and a slightly blueshift compared to ellagic acid emission intensity, they proposed that the emission arises as result of LMCT transitions. In this study, SU-101 exhibited a turn-on response toward both gaseous and H_2S dissolved in THF. Furthermore, the same turn-on response was observed even after the exposure to H_2S at 0.05 bar, see Fig. 12b. Remarkably, when SU-101 was exposed to water vapour and CO_2, the emission intensity of SU-101 did no showed significant changes, which indicates a good selectivity toward H_2S. Based on solution-state experiments (Fig. 12c), the LOD, for H_2S, showed a value of 22.16 ppm. The formation of polysulfides species was confirmed by XPS and Raman spectroscopy. Concerning the fluorescence detection mechanism, it was proposed that the formation of polysulfides rigidifies the MOF structure, decreasing molecular motions and internal
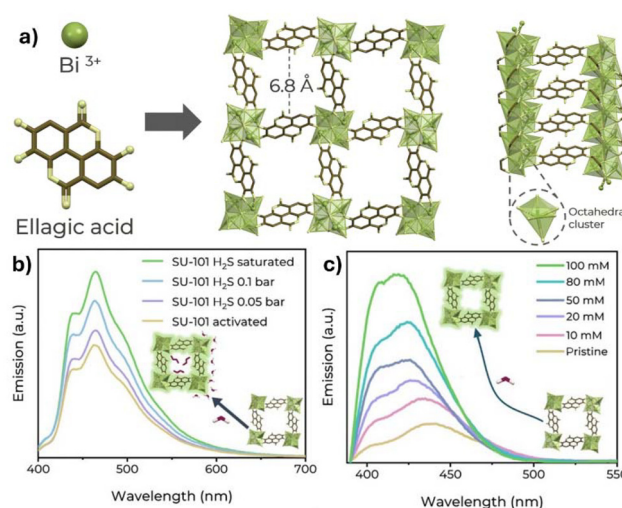

Fig. 12 (a) SU-101 chemical structure (carbon = brown, oxygen = yellow, Bi = green), (b) turn-on response of SU-101 towards H_2S in gas phase at different pressures, and (c) fluorescence response towards H_2S solved in THF (reproduced from ref. 71 licensed under CC 3.0).

vibrations, which reduces the non-radiative energy dissipation pathways. Also, polysulfides would limit the ligand-to-metal charge transfer, which are interrupted by the interaction of the polysulfides formed. The polysulfides act as electron donors toward the Bi(III) accepting centres. Such interaction would prevent the metal centre from accepting the charge coming from the ligand. Therefore, the LMCT becomes less efficient, favouring a greater amount of excited energy being released as light instead of dissipating through the ligand-to-metal charge transfer, therefore resulting in the turn-on effect of fluorescence after H_2S. The strategy employed in the use of SU-101 to detect H_2S was the transformation of hydrogen sulphide to polysulfides, knowing that SU-101 presents CUS as catalytic active sites. Here, polysulfides species have two functionalities: first they rigidify the framework structure, and second, they act as electron donor limiting the LMCT between linkers and Bi(III) centres.

The metal–organic frameworks Cu-MOF-74 and Co-MOF-74 were investigated by Sudarsan *et al.*,[72] who compared the effect of metal centres as well as the importance of charge transfer between the MOF structures and H_2S. Briefly, Sudarsan and coworkers dispersed both materials in water, which were put in contact with different analyte gases such as NH_3, H_2S, H_2, SO_2, and NO_2, finally, monitoring their fluorescence behaviour. Among the studied gases, for Cu-MOF-74, H_2S presented the best response (turn-on), with a LOD of 7 ppm, see Fig. 13a. On the other hand, Co-MOF-74 did not show significant responses toward these gases. Interestingly, Cu-MOF-74 exhibited responses at a wide range temperatures, *i.e.*, from 25 to 90 °C (Fig. 13b), which is something not common in previously reported MOFs. Regarding the Cu-MOF-74 fluorescence features, Cu-MOF-74 presents ligand-to-metal charge transfer transitions between organic linkers and Cu(II) centres. Such transitions hinder the intrinsic ligand fluorescence. Upon hydrogen sulphide addition, the Cu-MOF-74
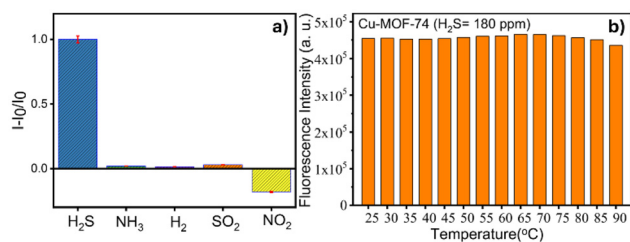
Fig. 13 (a) Selective Cu-MOF-74 fluorescent response towards H_2S, and (b) quasi-constant fluorescence intensity of Cu-MOF-74 upon exposure to H_2S at 180 ppm concentration (reproduced from ref. 72 Copyright 2025 with permission from John Wiley and Sons).
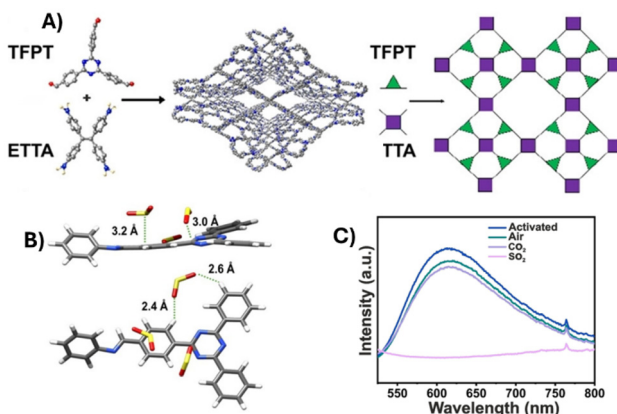

Fig. 14 Structure of SonoCOF-9, (b) SO_2 interactions with SonoCOF-9 (C = grey, O = red, N = blue, H = white, S = yellow), and (C) total quenching response towards SO_2 in gas phase (reproduced from ref. 74 Copyright 2024 with permission from John Wiley and Sons).

emission regenerates, which indicates that the LMCT interaction between linkers and Cu^{2+} ion in Cu-MOF-74 is prevented by H_2S. Concisely, Cu^{2+} ions show high propensity toward the S atoms, weakening ligand-Cu^{2+} electronic interactions. Since Co-MOF-74 does not present significant fluorescent response toward H_2S, it was suggested that Co-MOF-74 does not interact strongly with H_2S, which was corroborated by DFT calculations. Furthermore, they demonstrated that there was not electronic density transfer between Cu-MOF-74 and H_2S, contrary to NO_2, which induces electronic density transfer with Cu-MOF-74. Here, the detection strategy consisted in weakening the ligand-to-metal charge transfer between the organic linkers and the Cu(II) centres by the strong interaction of S–Cu and, as a consequence, regenerating the intrinsic ligand fluorescence. Additionally, Since Cu^{2+} ions show stronger affinity towards H_2S than Co^{2+} ions, Cu-MOF-74 demonstrates a better response. Thus, controlling MOF affinity towards H_2S could manage to design metal–organic frameworks with enhanced responses.

5. Emerging porous materials for SO_2 and H_2S detection

Additional to metal–organic frameworks, other emerging porous materials have been evaluated as fluorescent probes in order to detect both toxic gases. Herein we describe three selected examples of novel materials, i.e., covalent organic frameworks (COFs) and porous organic cages (POCs).

COFs are crystalline extended organic frameworks which are constructed by precisely integrating building blocks, via strong covalent bonds, into a two- or three-dimensional topology. Normally, COFs structures possess lightweight elements, such as C, H, B, N, and O atoms.[73] Due to strong covalent bonds in covalent organic frameworks, it is expected that these materials would show excellent chemical stability towards highly corrosive toxic gases, e.g., SO_2 and H_2S. Recently, Monti et al.[74] reported for the first time the use of a COF to detect and sense SO_2. Specifically, they studied a COF entitled SonoCOF-9, which is built up from 4,4′,4″-(1,3,5-triazine-2,4,6-triyl)tribenzaldehyde (TFPT) and 4,4′,4″,4‴-(ethene-1,1,2,2tetrayl)tetraaniline (ETTA) as building blocks, see Fig. 14a.

The calculated ΔH_{ads} (-42.3 kJ mol^{-1}), obtained by SO_2 adsorption–desorption isotherms, demonstrates stable adsorbed SO_2 on the walls of the COF material. Such ΔH_{ads} value is in good agreement with a relatively strong interaction of the SO_2 molecules with the π density from the rings and the lone pairs from the N atoms, i.e., ETTA building block (Fig. 14b), as revealed by reactive molecular dynamics simulations and Møller–Plesset perturbation theory calculations. In this case, SonoCOF-9 depicted a turn-off response after the exposure to SO_2 at 0.1 bar, where the emission intensity was almost fully quenched, compared to an activated control sample. Interestingly, other samples exposed to air and CO_2 did not present significant changes in the emission intensity (Fig. 14c). According to time-resolved photoluminescence experiments, they proposed that the decrease in emission intensity is due to a static quenching, i.e., the formation of a non-fluorescent complex in the basal state which hinder the $\pi^\star \rightarrow \pi$ transitions, which are responsible for the SonoCOF-9 photoluminescence. Finally, SonoCOF-9 exhibited an outstanding LOD, based on solution-state experiments, which value is 0.0064 ppm (6.4 ppb). In this case, SonoCOF-9 presented a remarkable fluorescent behaviour due to the highly conjugated systems of its building blocks. Additionally, the strong interaction between SonoCOF-9 and SO_2 molecules led to the formation of a non-fluorescent complex, which totally quenched the emission intensity of SonoCOF-9.

An intriguing example of the use of a COF to detect H_2S was introduced by Du and coworkers, where they use a Nanoscale Covalent Organic Framework (NCOF) to selectively sense hydrogen sulphide.[75] Concretely, Du et al. synthesised the NCOF based on 2,5-dihydroxyterephthalaldehyde (Dha) and tetra(pamino-phenyl)porphyrin (Tph), see Fig. 15a. Further, the NCOF was metallised with Cu^{2+}, which coordinates to nitrogen atoms from porphyrin ring, building up the COF entitled CuCOF (Fig. 15b). As depicted in Fig. 15c, the fluorescence intensity of NCOF is quenched after the formation of the Cu–N bonds in CuCOF since porphyrin coordinated to paramagnetic metal ions presents limited fluo-
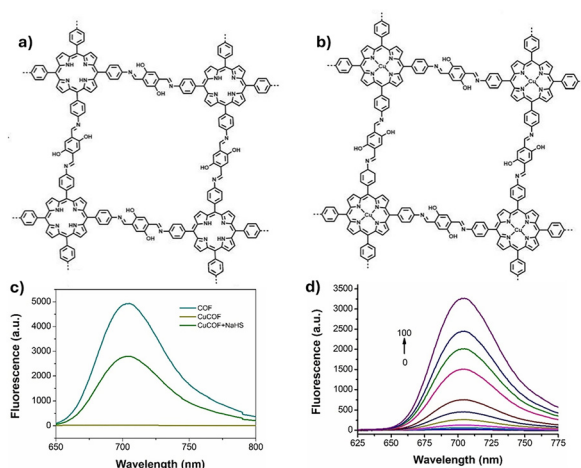
Fig. 15 The chemical structure of (a) NCOF, and (b) CuCOF. (c) Fluorescence spectra of no-metalated nanoCOF (COF), Cu-metalated nanoCOF (CuCOF), CuCOF upon interaction with NaHS (CuCOF + NaHS), and (d) turn-on response towards NaHS as function of NaHS concentration, from 0 to 100 μM. Reproduced from ref. 75 Copyright 2021 with permission from John Wiley and Sons.

rescence intensity. Nevertheless, upon the contact of CuCOF with NaHS (hydrogen sulphide source), the fluorescence intensity is recovered (Fig. 15c). In this case, the working principle to explain the fluorescence recovery of the NCOF is based on the fact that H_2S reacts with Cu^{2+} species and, thus, Cu^{2+} release the COF. Similar behaviour has been observed in PMOFs which possess Cu^{2+} coordinated to the porphyrin ring.[65] After the exposure of CuCOF to different NaHS concentrations, from 0 to 100 μM, the fluorescence spectra showed a turn-on response as function of NaHS concentration, establishing the limit of detection to be as low as 10 nM, see Fig. 15d. Lastly, the COF probe selectivity was investigated by measuring the fluorescence spectra of CuCOF exposed to different thiol and anionic species. The selectivity experiments indicate that CuCOF exhibit a turn-on response only in the presence of NaHS. In this example, the detection approach consists in using a covalent–organic framework based on porphyrin building block, which, due to the extended π-conjugated system, exhibits remarkable fluorescence features. Once constructed the NCOF, they chose Cu^{2+} cations to coordinate with porphyrin ring, since Cu^{2+} has demonstrated quenched phenomenon and selectively reactivity with H_2S, thus releasing Cu^{2+} species from the CuCOF, recovering the emission intensity (turn-on response).

Porous organic cages can be defined as discrete organic cages constructed by molecular building block units forming crystalline structures. POCs are built up mostly through covalent bonds, such as those between carbon–carbon or carbon–heteroatoms (e.g., imines, boronic esters, and amides) normally found in organic molecules. Conversely to extended porous frameworks, such as MOFs, POCs are synthesised and characterised initially as molecular species, and then assembled into materials in the solid state, attaining almost

all the advantages of emergent porous materials, i.e., high surface areas and pore volumes as well as open and tuneable pores.[76] In 2025 Liu and coworkers reported the use of a porous organic cage to sense, via fluorescence spectroscopy, hydrogen sulphide for the first time. Thus, Liu et al.[77] investigated a tertiary amine POC named 6FT-RCC3 that showed a remarkable H_2S capture (21.7 mmol g^{-1}), which, at this time, stands as the highest value reported at 25 °C and 1 bar for any adsorbent material. According to DFT calculations, the binding energy between 6FT-RCC3 and H_2S is −35.3 kJ mol^{-1}, and H_2S forms S–H⋯N hydrogen bond with the cage molecule, see Fig. 16a. 6FT-RCC3 exhibited a turn-on response after saturation with gaseous hydrogen sulphide, compared to an activated sample. Furthermore, the exposure of 6FT-RCC3 to water vapour, CO_2, NO_2, and SO_2 led to different fluorescent responses (Fig. 16b), showing that 6FT-RCC3 is a promising fluorescent probe with a good selectivity for H_2S. Regarding the fluorescence properties of 6FT-RCC3 and the detection phenomenon, 6FT-RCC3 contains imidazolidine rings, which possess a bipolar structure as result of the presence of two nitrogen atoms with different electronic properties, i.e., one acts as electron donor and the other one as an electron acceptor. Such electronic configuration grants intramolecular charge transfer, which is critical in luminescent properties. Additionally, since 6FT-RCC3 is only constructed with tertiary amine, the fluorescence is favoured in comparison to analogous POCs with primary and secondary amines, due to the absence of nitrogen-bonded hydrogens, and to the higher rigidification of the organic structure, assisting radiative excited-state deactivation. This was also corroborated by studying other secondary and primary amines POC materials. Interestingly, these POCs afforded lower responses toward H_2S. The turn-on response was suggested to arise as result of the rigidization of 6FT-RCC3 structure. Finally, the limit of H_2S detection obtained was calculated as low as 4.43 ppm, based on solution-state experiments. The detection approach employed here was the selection of a tertiary-based amine (6FT-RCC3), which, as consequence of its electronic properties, exhibited outstanding fluorescent features. Additionally, the hydrogen bonding between analyte molecules and amine groups allows the rigidification of the organic structure, enhancing the emission intensity.
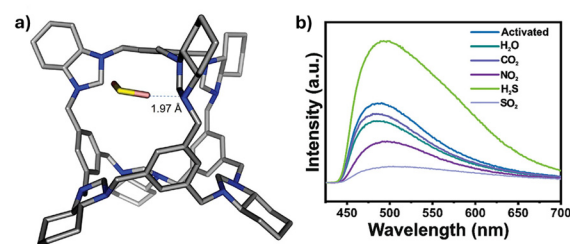

Fig. 16 (a) H_2S interaction with N atoms from 6FT-RCC3 crystal structure, and (b) 6FT-RCC3 fluorescence of activated samples and samples exposed to different gases (reproduced from ref. 77 Copyright 2024 with permission from John Wiley and Sons).

Finally, we believe that the use of COFs and POCs to detect highly corrosive toxic gases, such as SO_2 and H_2S, can have remarkable advantages over MOFs, particularly in terms of the chemical stability, and, due to their interesting fluorescence properties. Since the building blocks of covalent organic frameworks and porous organic cages, consist of purely organic units, these exhibit more and stronger π-conjugated systems, ideal for superior fluorescence features.

6.   Summary and outlook

Fluorescence spectroscopy has emerged as a promising analytical technique to sense different analytes. This technique shows several advantages above others, specifically, in terms of sample preparation, and sensitivity. Thus, the design and implementation of new materials which can be used as fluorescent probes toward distinct analytes is currently under active investigation. MOFs can show fluorescence due to π-conjugated systems by their organic ligands. Additionally, as the effect of coordination between ligands and metal centres, fluorescence can be considerably enhanced in MOF structures, in comparison to isolated organic ligands, since this ligand–metal bonding hinders vibrational modes found in pure ligands. Particularly for H_2S and SO_2, chemically stable MOFs can exhibit different chemical functionalities which directly interact with both polar gas molecules (*i.e.*, H_2S and SO_2). Then, MOFs can be tailored to possess specific functional groups, as well as defective sites, in order to obtain preferential adsorption sites to interact with H_2S and SO_2. Such interactions generally modify the electronic and vibronic structure of MOFs, leading to a change in the fluorescence features of these materials, which can be translated in a clear fluorescence response. Moreover, COFs, and POCs can also be used as successful probes for H_2S and SO_2 detection. These materials also exhibit some of the main advantages of MOFs, *e.g.*, permanent porosity, and high tuneability of their structures. However, since these fascinating supramolecular structures are not constructed with coordinative bonds, *i.e.*, they are purely ensembled *via* stronger covalent bonds, there are expected to be highly chemically stable toward both corrosive analytes. Interestingly, in these purely organic materials, amine groups demonstrated to play relevant roles in binding SO_2 and H_2S, as well as in the selective detection and sensing of both gases.

With these promising perspectives in mind, the utilisation of these novel materials, *i.e.*, MOFs, COFs, and POCs to detect and sense highly corrosive gases, paves the way to achieve novel devices for the detection and sensing of SO_2 and H_2S.

Author contributions

All authors contributed in writing the original draft and reviewing and editing the manuscript.

Conflicts of interest

There are no conflicts to declare.

Data availability

No primary research results, software or code have been included and no new data were generated or analysed as part of this review.

Acknowledgements

References

1 J. R. Lakowicz, *Principles of Fluorescence Spectroscopy*, Springer, Singapore, 3rd edn, 2006.

2 L. Basabe-Desmonts, T. J. J. Müller and M. Crego-Calama, *Chem. Soc. Rev.*, 2007, **36**, 993–1017.

3 D. Wu, A. C. Sedgwick, T. Gunnlaugsson, E. U. Akkaya, J. Yoon and T. D. James, *Chem. Soc. Rev.*, 2017, **46**, 7105–7123.

4 H. Furukawa, K. E. Cordova, M. O'Keeffe and O. M. Yaghi, *Science*, 2013, **341**, 1230444.

5 V. V. Butova, M. A. Soldatov, A. A. Guda, K. A. Lomachenko and C. Lamberti, *Russ. Chem. Rev.*, 2016, **85**, 280–307.

6 E. Martínez-Ahumada, M. L. Díaz-Ramírez, H. A. Lara-García, D. R. Williams, V. Martis, V. Jancik, V. Jancik, E. Lima and I. A. Ibarra, *J. Mater. Chem. A*, 2020, **8**, 11515–11520.

7 C. Healy, K. M. Patil, B. H. Wilson, L. Hermanspahn, N. C. Harvey-Reid, B. I. Howard, C. Kleinjan, J. Kolien, F. Payet, S. G. Telfer, P. E. Kruger and T. D. Bennett, *Coord. Chem. Rev.*, 2020, **419**, 213388.

8 E. Martínez-Ahumada, A. López-Olvera, V. Jancik, J. E. Sánchez-Bautista, E. González-Zamora, V. Martis, D. R. Williams and I. A. Ibarra, *Organometallics*, 2020, **39**, 883–915.

9 Y. Shan, G. Zhang, Y. Shi and H. Pang, *Cell Rep. Phys. Sci.*, 2023, **4**, 101301.

10 R. M. Guerrero, I. D. Lemir, S. Carrasco, C. Fernández-Ruiz, S. Kavak, P. Pizarro, D. P. Serrano, S. Bals, P. Horcajada and Y. Pérez, *ACS Appl. Mater. Interfaces*, 2024, **16**, 24108–24121.

11 J. Vazquez-Samperio, P. Acevedo-Peña, M. Goonzález M, M. Oliver-Tolentino, I. Padilla-Martínez, A. Guzmán-Vargas and E. Reguera, *Electrochim. Acta*, 2020, **346**, 1–12.

12 X. Tang, Y. Zhang, W. Sun and Y. Wang, *ACS Appl. Energy Mater.*, 2020, **3**, 11378–11387.

13 A. J. Rieth, A. M. Wright and M. Dincă, *Nat. Rev. Mater.*, 2019, **4**, 708–725.

14 E. Martínez-Ahumada, D. won Kim, M. Wahiduzzaman, P. Carmona-Monroy, A. López-Olvera, D. R. Williams, V. Martis, H. A. Lara-García, S. López-Morales, D. Solis-Ibarra, G. Maurin, I. A. Ibarra and C. S. Hong, *J. Mater. Chem. A*, 2022, **10**, 18636–18643.

15 E. D. Bloch, M. R. Hudson, J. A. Mason, S. Chavan, V. Crocellà, J. D. Howe, K. Lee, A. L. Dzubak, W. L. Queen, J. M. Zadrozny, S. J. Geier, L. C. Lin, L. Gagliardi, B. Smit, J. B. Neaton, S. Bordiga, C. M. Brown and J. R. Long, *J. Am. Chem. Soc.*, 2014, **136**, 10752–10761.

16 Z. Zhang, H. T. H. Nguyen, S. A. Miller, A. M. Ploskonka, J. B. Decoste and S. M. Cohen, *J. Am. Chem. Soc.*, 2016, **138**, 920–925.

17 Y. Cui, Y. Yue, G. Qian and B. Chen, *Chem. Rev.*, 2012, **112**, 1126–1162.

18 M. D. Allendorf, C. A. Bauer, R. K. Bhakta and R. J. T. Houk, *Chem. Soc. Rev.*, 2009, **38**, 1330–1352.

19 T. K. Pal, *Mater. Chem. Front.*, 2023, **7**, 405–441.

20 Y. Cai, T. Dong, Z. Bian, H. Liu, X. Liu and A. Liu, *Coord. Chem. Rev.*, 2025, **529**, 216470.

21 R. Dong, Z. Shen, H. Li, J. Cheng and Y. Fu, *J. Mater. Chem. C*, 2024, **12**, 12692–12707.

22 L. Bai, J. Wang, X. Ma and H. Lu, *Int. J. Environ. Res. Public Health*, 2018, **15**, 780.

23 Z. Meng, Y. Liu and D. Wu, *Inhalation Toxicol.*, 2005, **17**, 303–307.

24 M. D. Hartle and M. D. Pluth, *Chem. Soc. Rev.*, 2016, **45**, 6108–6117.

25 V. Balzani, P. Ceroni and A. Juris, *Photochemistry and Photophysics: Concepts, Research, Applications*, Wiley-VCH, Weinheim, 2nd edn, 2025.

26 T. C. Lovell, B. P. Branchaud and R. Jasti, *Eur. J. Org. Chem.*, 2024, **27**, e202301196.

27 Y. Y. Chia and M. G. Tay, *Dalton Trans.*, 2014, **43**, 13159–13168.

28 M. Stanisavljevic, S. Krizkova, M. Vaculovicova, R. Kizek and V. Adam, *Biosens. Bioelectron.*, 2015, **74**, 562–574.

29 M. L. Liu, B. Bin Chen, C. M. Li and C. Z. Huang, *Green Chem.*, 2019, **21**, 449–471.

30 I. Lignos, R. M. MacEiczyk, M. V. Kovalenko and S. Stavrakis, *Chem. Mater.*, 2020, **32**, 27–37.

31 M. Gouterman, *J. Mol. Spectrosc.*, 1961, **6**, 138163.

32 S. S. Rajasree, X. Li and P. Deria, *Commun. Chem.*, 2021, **4**, 47.

33 T. Wu, X. J. Gao, F. Ge and H. G. Zheng, *CrystEngComm*, 2022, **24**, 7881–7901.

34 R. Huang, Z. Yu, Z. Li, X. Lin, J. Hou, Z. Hu and J. Zou, *Coord. Chem. Rev.*, 2025, **526**, 216358.

35 S. Bej, X. Wang, J. Zhang, X. Yang and P. Ren, *Coord. Chem. Rev.*, 2024, **513**, 215862.

36 X. Chen, X. Zhang and Y. Zhao, *Chem. Soc. Rev.*, 2024, **54**, 152–177.

37 W. J. Newsome, S. Ayad, J. Cordova, E. W. Reinheimer, A. D. Campiglia, J. K. Harper, K. Hanson and F. J. Uribe-Romo, *J. Am. Chem. Soc.*, 2019, **141**, 11298–11303.

38 S. Nakamura, T. Mukai and M. Senoh, *Appl. Phys. Lett.*, 1994, **64**, 1687–1689.

39 T. H. Maiman, *Nature*, 1960, **187**, 493–494.

40 Y. Chen, W. Lu, M. Schröder and S. Yang, *Acc. Chem. Res.*, 2023, **56**, 2569–2581.

41 I. Strauss, A. Mundstock, D. Hinrichs, R. Himstedt, A. Knebel, C. Reinhardt, D. Dorfs and J. Caro, *Angew. Chem., Int. Ed.*, 2018, **57**, 7434–7439.

42 Y. Jiang and L. Heinke, *Langmuir*, 2021, **37**, 2–15.

43 B. H. Monjezi, S. Okur, R. Limbach, A. Chandresh, K. Sen, T. Hashem, M. Schwotzer, L. Wondraczek, C. Wöll and A. Knebel, *ACS Nano*, 2023, **17**, 6121–6130.

44 V. B. López-Cervantes, M. L. Martínez, J. L. Obeso, C. García-Carvajal, N. S. Portillo-Vélez, A. Guzmán-Vargas, R. A. Peralta, E. González-Zamora, I. A. Ibarra, D. Solis-Ibarra, J. L. Woodliffe and Y. A. Amador-Sánchez, *Dalton Trans.*, 2025, **54**, 1646–1654.

45 I. Jana, S. Naskar and D. Nandi, in *Journal of Physics: Conference Series*, Institute of Physics Publishing, 2020, vol. 1412.

46 D. Patel, D. Margolese and T. R. Dyke, *J. Chem. Phys.*, 1979, **70**, 2740–2747.

47 M. R. Milovavnović and S. D. Zarić, *ChemPlusChem*, 2025, e202400511.

48 A. A. A. Azzam, L. Lodi, S. N. Yurchenko and J. Tennyson, *J. Quant. Spectrosc. Radiat. Transfer*, 2015, **161**, 41–49.

49 Y. Zhao, L. Wu, K. Wu, R. J. Wei, H. Zeng, H. Pang, W. Lu and D. Li, *Coord. Chem. Rev.*, 2025, **524**, 216302.

50 E. Martínez-Ahumada, M. L. Díaz-Ramírez, M. de J. Velásquez-Hernández, V. Jancik and I. A. Ibarra, *Chem. Sci.*, 2021, **12**, 6772–6799.

51 Ü. Kökçam-Demir, A. Goldman, L. Esrafili, M. Gharib, A. Morsali, O. Weingart and C. Janiak, *Chem. Soc. Rev.*, 2020, **49**, 2751–2798.

52 J. N. Hall and P. Bollini, *React. Chem. Eng.*, 2019, **4**, 207–222.

53 W. Chen, Z. Wang, Q. Wang, K. El-Yanboui, K. Tan, H. M. Barkholtz, D. J. Liu, P. Cai, L. Feng, Y. Li, J. S. Qin, S. Yuan, D. Sun and H. C. Zhou, *J. Am. Chem. Soc.*, 2023, **145**, 4736–4745.

54 J. L. A. Jonathan and W. Steed, *Supramolecular Chemistry*, John Wiley & Sons Ltd, West Sussex, 3rd edn, 2022.

55 P. Brandt, A. Nuhnen, M. Lange, J. Möllmer, O. Weingart and C. Janiak, *ACS Appl. Mater. Interfaces*, 2019, **11**, 17350–17358.

56 R. M. Main, S. M. Vornholt, R. Ettlinger, P. Netzsch, M. G. Stanzione, C. M. Rice, C. Elliott, S. E. Russell, M. R. Warren, S. E. Ashbrook and R. E. Morris, *J. Am. Chem. Soc.*, 2024, **146**, 3270–3278.

57 N. L. Rosi, J. Kim, M. Eddaoudi, B. Chen, M. O'Keeffe and O. M. Yaghi, *J. Am. Chem. Soc.*, 2005, **127**, 1504–1518.

58 X. Cui, Q. Yang, L. Yang, R. Krishna, Z. Zhang, Z. Bao, H. Wu, Q. Ren, W. Zhou, B. Chen and H. Xing, *Adv. Mater.*, 2017, **29**, 1606929.

59 C. H. Hendon and A. Walsh, *Chem. Sci.*, 2015, **6**, 3674–3683.

60 C. Petit, B. Mendoza and T. J. Bandosz, *ChemPhysChem*, 2010, **11**, 3678–3684.

61 J. G. Flores, J. A. Zárate-Colín, E. Sánchez-González, J. R. Valenzuela, A. Gutiérrez-Alejandre, J. Ramírez, V. Jancik, J. Aguilar-Pliego, M. C. Zorrilla, H. A. Lara-García, E. González-Zamora, G. Guzmán-González, I. González, G. Maurin and I. A. Ibarra, *ACS Appl. Mater. Interfaces*, 2020, **12**, 18885–18892.

62 W. Cao, Y. Tang, Y. Cui and G. Qian, *Small Struct.*, 2020, **1**, 2000019.

63 J. X. Wang, J. Yin, O. Shekhah, O. M. Bakr, M. Eddaoudi and O. F. Mohammed, *ACS Appl. Mater. Interfaces*, 2022, **14**, 9970–9986.

64 L. Wang and Y. Chen, *Chem. Commun.*, 2020, **56**, 6965–6968.

65 Y. Ma, H. Su, X. Kuang, X. Li, T. Zhang and B. Tang, *Anal. Chem.*, 2014, **86**, 11459–11463.

66 T. T. Li, X. Zhang, Y. Wang, X. Zhang, H. Ren, B. C. Shiu and C. W. Lou, *Langmuir*, 2023, **39**, 14441–14450.

67 V. B. López-Cervantes, D. W. Kim, J. L. Obeso, E. Martínez-Ahumada, Y. A. Amador-Sánchez, E. Sánchez-González, C. Leyva, C. S. Hong, I. A. Ibarra and D. Solis-Ibarra, *Nanoscale*, 2023, **15**, 12471–12475.

68 P. Gao, S. Mukherjee, M. Zahid Hussain, S. Ye, X. Wang, W. Li, R. Cao, M. Elsner and R. A. Fischer, *Chem. Eng. J.*, 2024, **492**, 152377.

69 R. Dhir, M. Kaur and A. K. Malik, *J. Fluoresc.*, 2024, **35**, 1895–1917.

70 S. Carrasco, M. L. Martínez, Y. A. Amador-Sánchez, V. B. López Cervantes, E. Sánchez-González, N. S. Portillo-Vélez, R. A. Peralta, C. A. Celaya, A. Guzmán-Vargas, P. Horcajada, D. Solis-Ibarra and I. A. Ibarra, *Mater. Today Adv.*, 2025, **26**, 100579.

71 V. B. López-Cervantes, J. L. Obeso, J. G. Flores, A. Gutiérrez-Alejandre, R. A. Marquez, J. A. de los Reyes, C. V. Flores, N. S. Portillo-Vélez, P. Marín-Rosas, C. A. Celaya, E. González-Zamora, D. Solis-Ibarra, R. A. Peralta and I. A. Ibarra, *Chem. Sci.*, 2025, **16**, 5483–5492.

72 M. Shingole, S. Banerjee, B. Modak, S. Kolay, J. Mohanty and V. Sudarsan, *ChemPhotoChem*, 2025, **9**, e202400300.

73 O. M. Yaghi, M. J. Kalmutzki and C. S. Diercks, *Introduction to reticular chemistry: metal-organic frameworks and covalent organic frameworks*, Wiley-VCH, Weinheim, Germany, 1st edn, 2019.

74 W. Zhao, J. L. Obeso, V. B. López-Cervantes, M. Bahri, E. Sánchez-González, Y. A. Amador-Sánchez, J. Ren, N. D. Browning, R. A. Peralta, G. Barcaro, S. Monti, D. Solis-Ibarra, I. A. Ibarra and D. Zhao, *Angew. Chem.*, 2024, **137**, e202415088.

75 X. Ge, H. Zhang, C. Zhang and M. Du, *ChemNanoMat*, 2021, **7**, 530–533.

76 X. Yang, Z. Ullah, J. F. Stoddart and C. T. Yavuz, *Chem. Rev.*, 2023, **123**, 4602–4634.

77 J. L. Obeso, D. Hu, V. B. López-Cervantes, Y. A. Amador-Sánchez, C. V. Flores, J. G. Flores, S. Ling, E. Lima, A. Gutiérrez-Alejandre, M. A. Vera, R. A. Peralta, J. A. de los Reyes, D. Solis-Ibarra, I. A. Ibarra and M. Liu, *Small*, 2025, **21**, 2408155.